Thin Solid Films 562 (2014) 445–450

Contents lists available at ScienceDirect

Thin Solid Films

journal homepage: www.elsevier.com/locate/tsf

Formation of electrically conducting, transparent films using silver nanoparticles connected by carbon nanotubes

Sunna Hwang [a], Sun Young Noh [a], Heesuk Kim [a], Min Park [a], Hyunjung Lee [b,*]

[a] Polymer Hybrid Materials Research Center, Korea Institute of Science and Technology, Seoul 136-791, Republic of Korea
[b] School of Advanced Materials Engineering, Kookmin University, Jeongneung-dong, Seongbuk-gu, Seoul 136-702, Republic of Korea

ARTICLE INFO

Article history:
Received 11 November 2011
Received in revised form 13 March 2014
Accepted 18 March 2014
Available online 26 March 2014

Keywords:
Electrospinning
Carbon nanotubes
Bridging
Transparent conductive film
Silver fibrous microstructure

ABSTRACT

To achieve both optical transparency and electrical conductivity simultaneously, we fabricated a single-walled carbon nanotube (SWNT)/silver fiber-based transparent conductive film using silver fibers produced by the electrospinning method. Electrospun silver fibers provided a segregated structure with the silver nanoparticles within the fibrous microstructures as a framework. Additional deposition of SWNT/poly(3,4-ethylenedioxythiophene) doped with poly(styrenesulfonate) (PEDOT:PSS) layers resulted in a remarkable decrease in the surface resistance from very high value (>3000 kΩ/sq) for the films of electrospun silver fibers, without affecting the optical transmittance at 550 nm. The surface resistance of the SWNT/silver film after the deposition of three layers decreased to 17 Ω/sq with 80% transmittance. Successive depositions of SWNT/PEDOT:PSS layers reduced the surface resistance to 2 Ω/sq without severe loss in optical transmittance (ca. 65%). The transparent conductive films exhibited a performance comparable to that of commercial indium tin oxide films. The individual silver nanoparticles within the electrospun fibers on the substrate were interconnected with SWNTs, which resulted in the efficient activation of a conductive network by bridging the gaps among separate silver nanoparticles. Such a construction of microscopically conductive networks with the minimum use of electrically conductive nanomaterials produced superior electrical conductivity, while maintaining the optical transparency.

1. Introduction

Conventional transparent conductive thin films (TCFs) coated with metal oxides such as indium tin oxide (ITO) or zinc oxide are very brittle, and they easily form cracks. They are usually deposited by an uneconomical process, i.e., vacuum sputtering, while providing high electrical conductivity and high optical transparency in various optoelectric devices [1–5]. Thus, it is necessary to replace ITO with cost-effective materials that can easily form films over large area under practical conditions. Recent studies have shown the development of TCFs using carbonaceous materials (carbon nanotubes (CNTs), graphene, etc.), conducting polymers, and metal nanowires [6–13]. In particular, CNTs on glass or polymer substrates have been regarded as some of the most reliable candidates for TCF electrodes because of their extraordinary electrical, physical, and thermal properties [14–18]. Recently, promising results with considerably low sheet resistance (~100 Ω/sq) and high transmittance (>80% at 550 nm) have been reported for CNT-based TCFs [7,19–22]. However, the use of carbon materials cannot enable the simultaneous achievement of high electrical conductivity and high transparency because of the inverse relationship between the concentration of carbon materials and the sheet resistance. The current performance of carbon materials is still too poor for these materials to be used as substitutes for ITO.

A recent report states that the performance of a random mesh of metal nanowires exceeded that of a typical metal oxide; however, the mesh suffers from (a) inefficient transport paths of electrons and (b) substantial scattering of incident light when the nanowire density increases [23–25]. Interestingly, the researchers also observed that the transmittance of metal gratings was considerably superior to that of ITO at the same sheet resistance. Several research groups have attempted to demonstrate the use of metal gratings experimentally [26–28]. We addressed this issue by fabricating a silver fibrous microstructure using the electrospinning method. Recently, the combination of functional nanoparticles (metal or metal oxide) and polymer nanofibers has received considerable attention because alignment of these nanoparticles within nanofibers can have practical application for use as electrical conductive films [29–37].

In this study, we report a strategy to achieve optical transparency and sheet resistance comparable with those of ITO materials, by using electrospinning. Electrospun silver fibrous microstructure was used as

* Corresponding author. Tel.: +82 2 910 4662; fax: +82 2 910 4320.
E-mail address: hyunjung@kookmin.ac.kr (H. Lee).

http://dx.doi.org/10.1016/j.tsf.2014.03.066
0040-6090/

a conductive frame for the deposition of an ultra-thin film of single-walled carbon nanotubes (SWNTs)/poly-(3,4-ethylenedioxythiophene) doped with poly(styrenesulfonate) (PEDOT:PSS). In order to reduce the scattering effect from a silver frame and enhance the optical transmittance, a minimum number of silver nanoparticles that formed a fibrous structure were produced, and a thin film of SWNT/PEDOT:PSS was linked with conductive silver domains on the substrate. These films exhibited a very low sheet resistance of ~17 Ω/sq with ~80% optical transparency. The resistance of these films increased up to 26 Ω/sq (~50%) in four months, which was staying still at the same order of the initial resistance in the air.

2. Experimental details

2.1. Materials

Silver nitrate ($AgNO_3$, 99+%, ACS reagent) and polyvinylpyrrolidone (PVP, Mw = 1,300,000) were purchased from Sigma-Aldrich Co. SWNTs were purchased from Hanwha Nanotech Co., Ltd. (an Arc-discharge process), and poly(3,4-ethylenedioxythiophene)/poly(styrenesulfonate) (PEDOT:PSS) solution was purchased from Baytron® Co.

In order to prepare electrospinning solutions of $AgNO_3$ and PVP, 2.5 g of $AgNO_3$ was dissolved in 2 ml of acetonitrile in a 10-ml vial by stirring for 30 min, and 0.5 g of PVP powder was dissolved in 5 ml of ethanol by stirring for 2 h. The $AgNO_3$ and PVP solutions were then mixed and stirred for 1 h. Thus, we prepared a homogeneous and viscous solution for electrospinning [34,38].

2.2. Electrospinning process

The setup for electrospinning comprised a high-voltage supply, a pressure gauge to measure nitrogen-gas pressure, a syringe with a metal tip, and a flat collector. Voltage of 20 to 25 kV was applied to this solution. The electrospinning solution was poured into a 30-ml syringe attached to a metal tip with a 22 gauge size (needle diameter: ca. 0. 64 mm) and was pushed at a nitrogen-gas pressure of 0.01 MPa. The tip-to-collector distance was 15 cm. The nanofibers formed on the quartz glass were calcined at 200 °C for 2 h and subsequently at 300 °C for 1 h in an air atmosphere at a heating rate of 10 °C/min.

2.3. Deposition of SWNT/PEDOT:PSS

In order to deposit the solution mixture of SWNT/PEDOT:PSS on an electrospun silver-fiber-coated quartz glass, SWNTs that were sonicated using a horn-type sonicator (330 W) were dispersed in dimethylformamide. Then, 3 ml of PEDOT:PSS solution was added to an SWNT-dispersed solution. The mixture was then sonicated for 30 min. A droplet of SWNT/PEDOT:PSS solution was placed on the silver-fiber-coated quartz glass and then was dried at room temperature. The deposition process of SWNT/PEDOT:PSS was repeated 3, 5, 7 and 9 times, respectively. A overall process for the fabrication of a transparent conductive film using a silver fibrous microstructure and SWNT/PEDOT:PSS layers is summarized in Fig. 1.

2.4. Characterization

The surface morphology of the films was observed by using field-emission scanning electron microscopes (FE-SEM, JSM-6701F, JEOL, Japan and FE-SEM, Hitachi S-4100, Hitachi, Japan). The operating voltage in SEM was 10–15 kV. The crystal structures of silver crystals were observed on an X-ray diffraction (XRD, D/MAX-2500, Rigaku International Co., Japan) with a graphite monochromator and Cu Kα radiation (λ = 0.154 nm) and focusing/parallel-beam configurations The scanning speed was 4°/min over the range from 20° to 100°. The film transmittance was measured with a UV/Vis/NIR spectrophotometer (V-670, Jasco International Co., Ltd., Japan). The electrical conductivity was measured using a Keithley Model 2182A nanovoltmeter and Keithley Model 6220 power source in a four-point probe set-up at room temperature. Atomic force microscopy (AFM) images of the LBL thin films were recorded under room temperature in a commercial AFM (Asylum Research MFP3D) in noncontact mode (alternating current (AC) mode) with 10 nm standard cantilevers (AC160TS, Olympus). cAFM imaging was performed using the ORCA module (Asylum Research MFP-3D) in noncontact mode with a doped Si tip, Electri-Lever (AC240TM, Olympus).

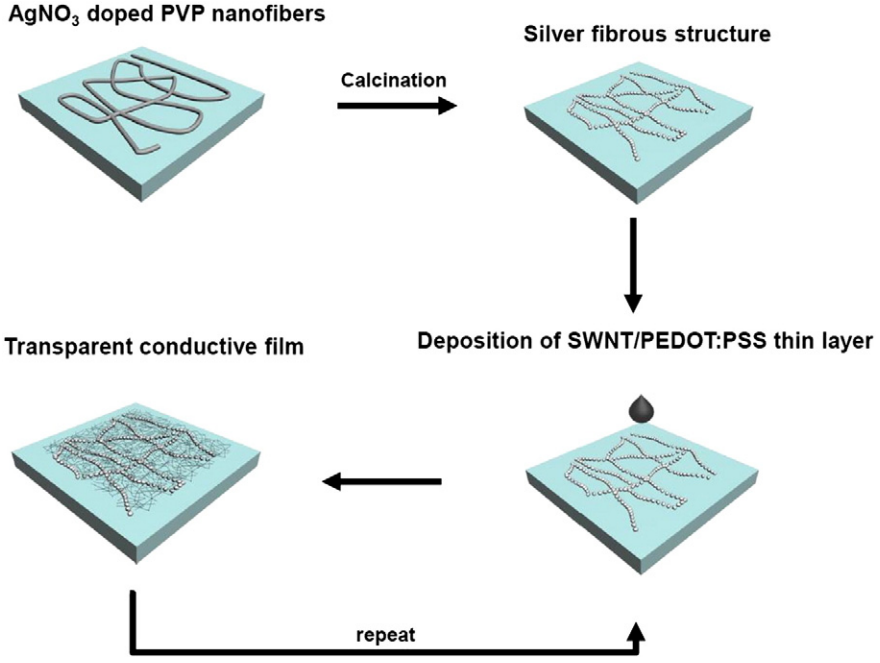

Fig. 1. Schematic representation of the fabrication of a transparent conductive film using a silver fibrous microstructure and a SWNT/PEDOT:PSS film. Detailed methods were described in the Experimental details section.

The sample bias was applied to the silver electrode coated on the multi-layered film via a wire from the ORCA holder.

3. Results and discussion

The morphologies of films based on a silver fibrous microstructure and SWNT/PEDOT:PSS layers were observed at each step in Fig. 1 and they are shown in Fig. 2. Although silver is very conductive in the bulk form, there are limitations in metal-based transparent conductive films. Higher-density metal nanowires or thicker metal films (of a certain thickness) are required to achieve higher electrical conductivity in TCFs. However, these result in an undesirable decrease in optical transparency.

In this study, we expected that the transparency could be improved by manipulating the silver particles into forming a fibrous structure and that the conductivity could be improved by combining the silver conductive domains with SWNTs. Using a solution mixture of $AgNO_3$ and PVP, we first produced $AgNO_3$-doped PVP fibers on quartz glass by electrospinning. The $AgNO_3$/PVP fibers were then coated randomly and uniformly on the substrate. Finally, the fibers were calcined to remove PVP and obtain a fibrous microstructure of silver. Low- and high-magnification SEM images for $AgNO_3$/PVP fibers before and after thermal calcination are shown in Fig. 2a and b, respectively. The presence of crystalline silver was confirmed by XRD analysis (see inset in Fig. 2b). XRD pattern shows a crystalline silver structure. The strong diffraction peaks at 2θ values of 38.10°, 44.25°, 64.43°, and 77.28° correspond to (111), (200), (220), and (311) lattice planes, respectively, thereby indicating the formation of crystalline silver (JCDPS, card no 04-0783). A close look at the silver fibrous microstructure (Fig. 2b) showed that the silver fiber consisted of discontinuously laid silver domains due to the local growth of crystalline silver domains during thermal sintering. We aimed at minimizing the amount of silver

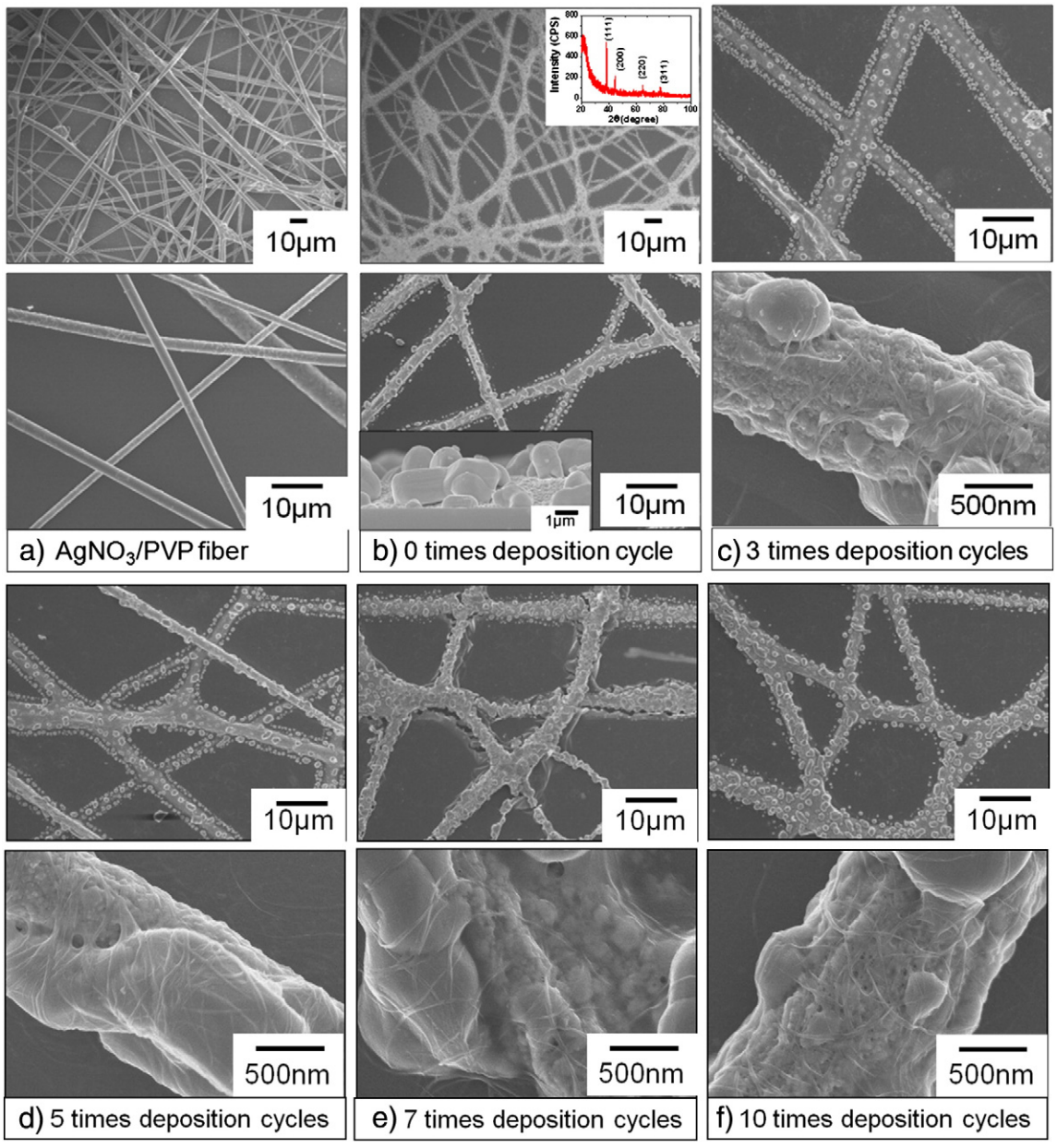

Fig. 2. Scanning electron microscope images for (a) silver nitrate/PVP nanofibers, (b) silver nanofibers after thermal calcination, and (c–f) silver fibrous microstructures with 3, 5, 7, and 10 SWNT/PEDOT:PSS layers at low and high magnifications. The inset in (b) shows the cross-sectional image of discontinuously laid silver particles after calcination. The insets in (b) show XRD analyses of the silver fibrous microstructure produced by an electrospinning technique and followed by thermal treatment and the cross-sectional image of discontinuously laid silver particles after calcinations, respectively.

particles on the substrate by controlling the electrospinning time in order to maintain the transparency. Then, the SWNT/PEDOT:PSS layer was spin-coated up to 10 deposition cycles on silver fibrous microstructures and was linked together with stepping silver conductive domains on the substrate. SWNTs and PEDOT:PSS covered the silver fibrous microstructures effectively (Fig. 2c, d, e, and f). High electrical conductivity and transparency of more than 80% was achieved because the SWNTs bridged the conductive silver particles.

We monitored the effect of the SWNT/PEDOT:PSS layers on surface resistance and transmittance with increasing number of SWNT/PEDOT:PSS layers (3, 5, 7, and 10 layers) deposited on the silver fibrous microstructure. The corresponding photographs of TCFs are shown in Fig. 3a. The electrical and optical properties of TCFs as a function of the number of layers of SWNT/PEDOT:PSS are summarized in Table 1. In a silver fibrous film without SWNT/PEDOT:PSS layers, the surface resistance was a considerably large value of more than 3000 kΩ/sq, and the transmittance was maintained at 81% at 550 nm (Fig. 3b). The small number of silver particles on the substrate resulted in a large electrical resistance as well as high optical transparency. We then introduced layers of SWNTs/PEDOT:PSS. As the number of SWNTs/PEDOT:PSS layers increased, the overall color of the films changed to dark blue because of the presence of PEDOT:PSS; further, thick black structures, which were SWNT-covered silver fibers, were found easily in a film (Fig. 3a). After the third SWNT/PEDOT:PSS layer was deposited, the surface resistance of the film dramatically decreased to 17 Ω/sq, while the optical transmittance remained almost unchanged (ca. 80%). This conductivity value of the silver/SWNT/PEDOT:PSS film is similar to that of an ITO film. By repeated deposition of SWNT/PEDOT:PSS layers, we observed that the surface resistance decreased continuously because of the increasing surface coverage by SWNT/PEDOT:PSS, which obeyed a typical power law as a function of the conductive filler fraction (given below), which was predicted by the standard percolation theory [39–43].

$$R \propto (V - V^*)^{-p} \quad (1)$$

Table 1
Electrical and optical properties of silver nanofiber films as a function of the number of SWNT/PEDOT:PSS layers.

Number of deposition cycles	0	3	5	7	10
Silver/SWNT					
Transmittance (%)	81	77	71	67	61
Surface resistance (Ω/sq)	$>3 \pm 30 \times 10^6$	18 ± 2	13 ± 3	8 ± 2	3 ± 1
Silver/SWNT/PEDOT:PSS					
Transmittance (%)	81	80	75	71	65
Surface resistance (Ω/sq)	$>3 \pm 30 \times 10^6$	17 ± 2	13 ± 2	4 ± 1	2 ± 0.5

where R is the surface resistance, V is the volume fraction of fillers, V* is the critical volume fraction of the filler associated with the percolation threshold and p is a critical exponent which depends on the dimensionality of the space involved. The theoretical values of *p* are 1.33 for a 2D percolation network and 1.94 for a 3D percolation network [13]. By assuming that the volume fraction of SWNTs is proportional to the number of deposited layers, we used the number of deposited layers instead of the volume fraction of fillers because of the uncertainties regarding the CNT concentration. The last four experimental points in Fig. 3b were fitted to this relationship, and the value of p was found to be approximately 1.81 with PEDOT:PSS and 1.44 without PEDOT/PSS. Fig. 3c shows a reasonably accurate fitting in the log–log scale plot of the Eq. (1), and it shows that the change in surface resistance with the number of layers of SWNT/PEDOT:PSS can be explained by the construction of percolation networks using SWNTs. It also indicated that the silver/CNT film with PEDOT:PSS is close to the value predicted for the 3D theoretical model and the other is quite close to that for the 2D model. Overall these films have an intermediate character between that for 2D ($p = 1.33$) and 3D ($p = 1.94$). The robust decrease in surface resistance could be attributed to the combined effect of a silver fibrous microstructure and SWNT/PEDOT:PSS layers. The individual silver nanoparticles within the electrospun fibrous microstructure on the substrate were connected to the SWNTs, which results in the effective activation of a conductive network by bridging the gaps between the separate silver nanoparticles and SWNTs (Fig. 1). Tokuno T et al.

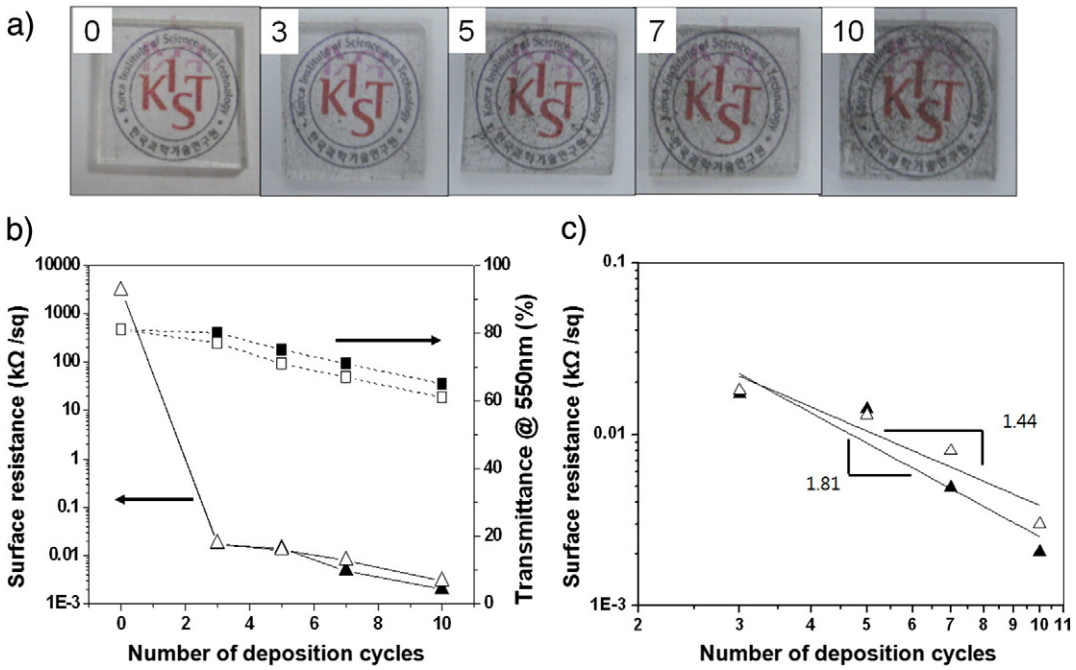

Fig. 3. (a) Photographs of transparent conductive silver/CNT hybrid films with increasing number of layers (0, 3, 5, 7, and 10) of SWNT/PEDOT:PSS (from left to right). The substrate size is 1×1 cm^2. (b) The change in the electrical resistance and transmittance of the silver/CNT hybrid films as a function of the number of SWNT (open symbol) or SWNT/PEDOT:PSS (close symbol) layers. (c) The log–log scale plot of panel (b).

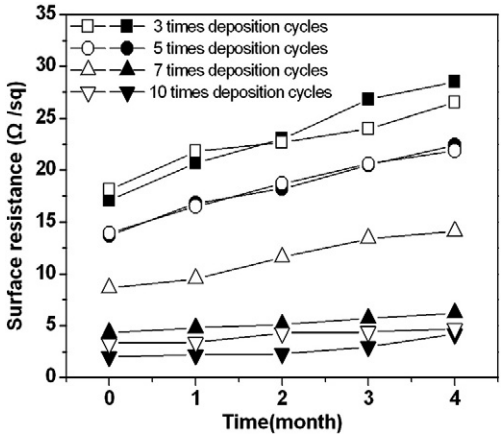

Fig. 4. The effect of the number of deposited layers on the stability of the surface resistance in silver/CNT hybrid films. The open symbols mean silver/SWNT and the close symbols mean SWNT/PEDOT:PSS hybrid films.

reported recently that hybrid transparent electrodes with silver nanowires and SWNTs exhibited a sheet resistance of 29.2 Ω/sq with a transparency of 80% [44]. Compared with this value, the hybrid system in this study exhibited lower sheet resistance with a similar transparency (a sheet resistance of 17.0 Ω/sq with a transparency of 80%).

The change in the optical transmittance was similar to that in the electrical conductivity, and it decreased up to 65%. As well known, PEDOT:PSS is one of the most stable materials among the conducting polymers. However, PEDOT:PSS materials are hydroscopic in the air and their electrical conductivities decrease due to the severe water uptake [45–47]. We needed to check the stability of PEDOT:PSS in the air. In order to confirm the long-term stability of silver/CNT hybrid films, we monitored the surface resistance when the films were exposed to air at room temperature for several months (Fig. 4). We found that their resistivities were not increasing more than twice than their initial values and they were lower than 30 Ω/sq in all samples even though there was a disadvantage for the water adsorption of the PEDOT:PSS. Especially the resistivity of the silver/CNT hybrid films remained below 5 Ω/sq for four months when 10 SWNT/PEDOT:PSS layers were deposited. We found that silver fibrous structure disappeared in several weeks without additional deposition of CNTs and they transformed into other stable crystalline structures such as large cubic particles. We combined the silver nanoparticles and carbon nanotubes. It suppressed the migration of silver nanoparticles. Finally, it showed a long stability over several months.

PEDOT:PSS is a typical material that is used as a dispersing agent of SWNTs, and it is well known for decreasing the contact resistance between SWNTs because of its high electrical conductivity [48–50]. When we attempted the same procedure using an SWNT-dispersed solution without PEDOT:PSS, we found that the surface resistance of the silver/SWNT films was slightly higher than that of TCFs with PEDOT:PSS at the same transmittance (Fig. 3b). The exponent in the log–log scale plot was approximately 1.44, which was smaller than that with PEDOT:PSS. This implies that the surface resistances of films with PEDOT:PSS decrease faster than those without PEDOT:PSS as the loading amount of SWNTs increases (Fig. 3c).

We compared the surface morphologies of TCFs with and without PEDOT:PSS via atomic force microscopy (AFM) (Fig. 5). AFM provides useful information about the morphology in the height scan and the current map of composite films in the conductive mode, which explain how current paths are formed in silver/CNT hybrid films [7,22,51]. In order to obtain the superior resolution of the nanotubes, the micron-

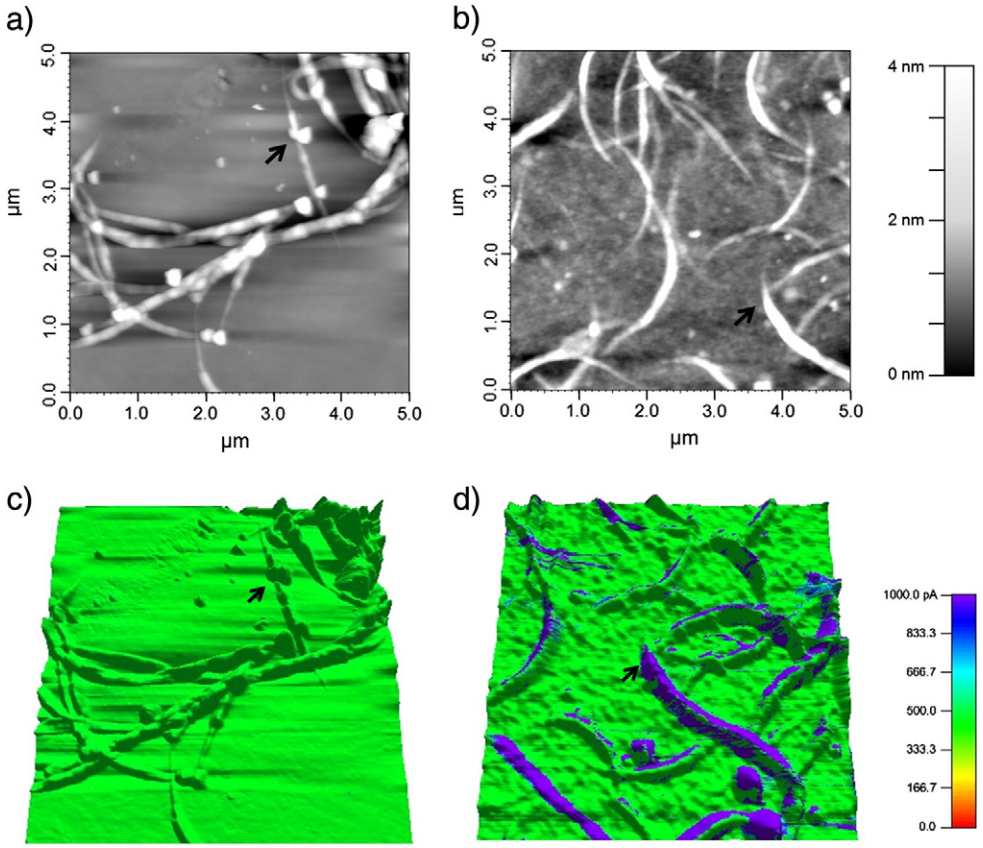

Fig. 5. AFM images with height mode presenting the topography of (a) silver/SWNT and (b) silver/SWNT/PEDOT:PSS hybrid films. (c) and (d) represent AFM images with current channel overlays on the topography shown in panels (a) and (b). The image size is 5 μm × 5 μm. The black arrows represent the same position in each sample, respectively, which were added for eye's guideline in comparing these.

sized silver fibrous microstructure was avoided while scanning images, and the interstitial area between the silver fibers was observed by using both tapping and conductive modes in AFM. The white region in Fig. 5a and b indicates the height of SWNT with or without PEDOT:PSS. Without PEDOT:PSS, aggregated or bundled SWNTs were easily found (Fig. 5a), and the overall electrical conductivity was very low around 400 pA at the bias voltage of 100 mV (Fig. 5c). Further, the optical transmittance without PEDOT:PSS was lower than that with PEDOT:PSS. This could be attributed to the many aggregates or bundles of nanotubes even though the same volume of dispersion solution was transferred on the substrate for the same number of deposited layers, both with and without PEDOT:PSS (Fig. 3b). Also PEDOT:PSS helps to disperse the nanotubes, leading to higher transmittance [52]. These aggregated nanotubes didn't provide effective paths for electron transport and there were no differences between nanotubes and the bare substrate in Fig. 5c. However, there is still a conductive path on a substrate. As you can image from Fig. 1, there is a very thin film consisting of well dispersed SWNTs on a substrate. Usually the diameter of one SWNT is a few nanometers (c.a. <5 nm), which was not easy to be seen in a 5 μm × 5 μm image. These well dispersed SWNTs would contribute to a weak current on a bare substrate. That's the reason why there is still a conductive path on the bare substrate. On the other hand, SWNTs with PEDOT:PSS showed highly dispersed nanotubes (Fig. 5b) and they formed percolating networks, which resulted in improved electrical conductivity (over 1000 pA) at the same bias voltage (Fig. 5d). In particular, percolated conductive pathways were observed by following the nanotubes. This means that PEDOT:PSS is expected to decrease the contact resistance between nanotubes. The PEDOT:PSS is always used on ITO to help with the interface and good contact resistances to the polymer films. Therefore PEDOT:PSS provides good interface between our TCF and the organic active layers in organic photovoltaic devices and organic light-emitting diodes in the future. By forming a minimum number of micron-sized (diameter) silver fibers and controlling the loading density of SWNTs, we can achieve higher electrical conductivity without a severe loss of optical transparency. Further, these silver/CNT hybrid transparent conductive films are applicable to the photonics industries, i.e., in solar cells, smart windows, optoelectric devices, and so on, in the near future.

4. Conclusions

We demonstrated the use of silver fiber microstructure in TCFs with the aid of SWNT/PEDOT:PSS, and we monitored the electrical and optical properties of the films by depositing SWNT/PEDOT:PSS layers. This study showed that the electrical properties in a fibrous structure of silver particles can be dramatically enhanced by the deposition of SWNT/PEDOT:PSS layers, while the optical transmittance was kept insensitive to the existence of SWNTs after the deposition of three layers. After more than three consecutive deposition cycles, the transmission dropped by 15%. Such a behavior can be attributed to the formation of a conductive network in which SWNTs bridge the gaps between separate silver nanoparticles in the fibrous microstructure; this makes it possible to improve electrical property and maintain superior transmittance. The low-cost/large-scale production by electrospinning which exhibits low toxicity and the high performance comparable to those of ITO glass makes the silver fibrous microstructure a promising candidate to be used in the fabrication of a wide variety of electronic devices. Finally, we strongly anticipate that the optical properties of the silver fibrous microstructure can be considerably improved by using a fibrous microstructure made of a subwavelength-sized silver framework and by varying the feed materials and their concentrations in the electrospinning process.

Acknowledgment

We thank Dr. Junkyung Kim, Dr. Soonho Lim, Dr. Min Park, and Dr. Sang-soo Lee for their useful discussions. Further, we thank Kyoung Ah Oh and Min Ah Kim for their assistance in performing the experiment. This work was supported by the National Research Foundation of Korea (NRF) grant funded by the Korean government (MEST) (No. 2012R1A2A2A01014288, NRF-2011-0014376 and NRF-2009-C1AAA001-0093049).

References

[1] R.C. Darran, P.W. Richard II, K.S. Daniel, M.S. Suzanne, C.P. David, P.C. Gregory, R.R. Newton, Appl. Phys. Lett. 76 (11) (2000) 1425.
[2] G. Gruner, J. Mater. Chem. 16 (35) (2006) 3533.
[3] Y. Hu, X. Diao, C. Wang, W. Hao, T. Wang, Vacuum 75 (2) (2004) 183.
[4] N. Saran, K. Parikh, D.-S. Suh, E. Munoz, H. Kolla, S.K. Manohar, J. Am. Chem. Soc. 126 (14) (2004) 4462.
[5] J. Shin, P.V. Braun, W. Lee, Sensors Actuators B Chem. 150 (2010) 183.
[6] J.-Y. Lee, S.T. Connor, Y. Cui, P. Peumans, Nano Lett. 8 (2) (2008) 689.
[7] D. Zhang, K. Ryu, X. Liu, E. Polikarpov, J. Ly, M.E. Tompson, C. Zhou, Nano Lett. 6 (9) (2006) 1880.
[8] J.S. Moon, J.H. Park, T.Y. Lee, Y.W. Kim, J.B. Yoo, C.Y. Park, J.M. Kim, K.W. Jin, Diamond Relat. Mater. 14 (11–12) (2005) 1882.
[9] N. Ferrer-Anglada, M. Kaempgen, V. Skakalova, U. Dettlaff-Weglikowska, S. Roth, Diamond Relat. Mater. 13 (2) (2004) 256.
[10] V.C. Tung, L.-M. Chen, M.J. Allen, J.K. Wassei, K. Nelson, R.B. Kaner, Y. Yang, Nano Lett. 9 (5) (2009) 1949.
[11] S. De, T.M. Higgins, P.E. Lyons, E.M. Doherty, P.N. Nirmalraj, W.J. Blau, J.J. Boland, J.N. Coleman, ACS Nano 3 (7) (2009) 1767.
[12] B.-S. Kim, K.-D. Suh, B. Kim, Macromol. Res. 16 (2008) 76.
[13] A.R. Madaria, A. Kumar, F.N. Ishikawa, C. Zhou, Nano Res. 3 (8) (2010) 564.
[14] R.H. Baughman, A.A. Zakhidov, W.A. de Heer, Science 297 (5582) (2002) 787.
[15] S.J. Tans, A.R.M. Verschueren, C. Dekker, Nature 393 (6680) (1998) 49.
[16] J. Kong, N.R. Franklin, C. Zhou, M.G. Chapline, S. Peng, K. Cho, H. Dai, Science 287 (5453) (2000) 622.
[17] G. Viswanathan, N. Chakrapani, H. Yang, B. Wei, H. Chung, K. Cho, C.Y. Ryu, P.M. Ajayan, J. Am. Chem. Soc. 125 (31) (2003) 9258.
[18] K. Kim, S.J. Cho, S.T. Kim, I.-J. Chin, H.J. Choi, Macromolecules 38 (26) (2005) 10623.
[19] M.-S. Jung, T.-L. Choi, W.-J. Joo, J.-Y. Kim, I.-T. Han, J.M. Kim, Synth. Met. 157 (22–23) (2007) 997.
[20] B.P. Bhavin, F. Giovanni, E. Goki, C. Manish, Appl. Phys. Lett. 90 (12) (2007) 121913.
[21] H.-Z. Geng, K.K. Kim, K.P. So, Y.S. Lee, Y. Chang, Y.H. Lee, J. Am. Chem. Soc. 129 (25) (2007) 7758.
[22] W.R. Michael, A.T. Mark, D.M. Michael, P. Hans-Jurgen, D. Gilles, S. Niyazi Serdar, H. Liangbing, G. George, Appl. Phys. Lett. 88 (23) (2006) 233506.
[23] C. Woo-Sung, L. Hyeon-Jae, L. Yang-Doo, P. Jung-Ho, K. Jai-Kyeong, L. Yun-Hi, J. Byeong-Kwon, IEEE Electron Device Lett. 28 (5) (2007) 386.
[24] T.A. Walsh, L. Shawn-Yu, IEEE Electron Device Lett. 55 (5) (2008) 1101.
[25] G. Landis, P. Younger, IEEE Trans. Compon. Hybrids Manuf. Technol. 2/3 (1979) 350.
[26] Y. Hiroshi, H. Yuji, M. Yasutaka, I. Kuniharu, S. Masatsugu, Macromol. Symp. 267 (1) (2008) 100.
[27] S. Hong-Yi, L. Zhi-Yuan, G. Ben-Yuan, J. Appl. Phys. 97 (3) (2005) 033102.
[28] H.-C. Lee, J.-Y. Kim, C.-H. Noh, K.Y. Song, S.-H. Cho, Appl. Surf. Sci. 252 (8) (2006) 2665.
[29] H. Mickael, B. Kristopher, K. Guzeliya, G. Yury, Adv. Funct. Mater. 18 (16) (2008) 2322.
[30] Z.-M. Huang, Y.Z. Zhang, M. Kotaki, S. Ramakrishna, Compos. Sci. Technol. 63 (15) (2003) 2223.
[31] D. Li, Y. Xia, Adv. Mater. 16 (14) (2004) 1151.
[32] J. Bai, Y. Li, M. Li, S. Wang, C. Zhang, Q. Yang, Appl. Surf. Sci. 254 (15) (2008) 4520.
[33] N.A.M. Barakat, K.-D. Woo, M.A. Kanjwal, K.E. Choi, M.S. Khil, H.Y. Kim, Langmuir 24 (20) (2008) 11982.
[34] W.-J. Jin, H.J. Jeon, J.H. Kim, J.H. Youk, Synth. Met. 157 (10–12) (2007) 454.
[35] Y. Wang, Q. Yang, G. Shan, C. Wang, J. Du, S. Wang, Y. Li, X. Chen, X. Jing, Y. Wei, Mater. Lett. 59 (24–25) (2005) 3046.
[36] X.Z., Ming Jin, Shunsuke Nishimoto, Zhaoyue Liu, T.M., A.F., Donald A. Tryk, Nanotechnology 18 (7) (2007) 075605.
[37] W. Lee, H. Kim, H. Lee, J. Membr. Sci. 320 (2008) 78.
[38] S. Lee, G.D. Moon, U. Jeong, J. Mater. Chem. 19 (6) (2009) 743.
[39] X. Zhao, A.A. Koos, B.T.T. Chu, C. Johnston, N. Grobert, P.S. Grant, Carbon 47 (3) (2009) 561.
[40] L. Jiantong, Z. Zhi-Bin, Z. Shi-Li, Appl. Phys. Lett. 91 (25) (2007) 253127.
[41] D. Simien, J.A. Fagan, W. Luo, J.F. Douglas, K. Migler, J. Obrzut, ACS Nano 2 (9) (2008) 1879.
[42] S. Soliveres, J. Gyani, C. Delseny, A. Hoffmann, F. Pascal, Appl. Phys. Lett. 90 (8) (2007) 082107.
[43] L. Hu, D.S. Hecht, G. Gruner, Nano Lett. 4 (12) (2004) 2513.
[44] T. Tokuno, M. Nogi, J. Jiu, K. Suganuma, Nanoscale Res. Lett. 7 (1) (2012) 281.
[45] J. Huang, P.F. Miller, J.C. de Mello, A.J. de Mello, D.D.C. Bradley, Synth. Met. 139 (2003) 569.
[46] J. Huang, P.F. Miller, J.S. Wilson, A.J.d. Mello, J.C.d. Mello, D.D.C. Bradley, Adv. Funct. Mater. 15 (2005) 290.
[47] H.-E. Yina, C.-F. Leed, W.-Y. Chiua, Polymer 52 (22) (2011) 5065.
[48] H.T. Ham, Y.S. Choi, M.G. Chee, M.H. Cha, I.J. Chung, Polym. Eng. Sci. 48 (1) (2008) 1.
[49] J. Roderick, D. Benoit, J. Rishabh, K. Bernard, G. Samuel, Adv. Funct. Mater. 18 (17) (2008) 2548.
[50] M. Kalb, L. Kavan, M.a. Zukalov, L. Dunsch, Carbon 45 (7) (2007) 1463.
[51] H.J. Park, K.A. Oh, M. Park, H. Lee, J. Phys. Chem. C 113 (30) (2009) 13070.
[52] S.-H. Jo, Y.-K. Lee, J.-W. Yang, W.-G. Jung, J.-Y. Kim, Synth. Met. 162 (13–14) (2012) 1279.